DEFORMATION MECHANISMS AND FATIGUE BEHAVIOR OF PRESTRAINED INCONEL 718 SUPERALLOY

Sreeramesh Kalluri[1], K. Bhanu Sankara Rao[2], Gary R. Halford[3], and Michael A. McGaw[4]

[1]NYMA, Inc.
NASA Lewis Research Center
Cleveland, Ohio 44135
[2]Previously Research Associate of NRC - NASA Lewis Research Center
Cleveland, Ohio 44135
Presently, Materials Development Division, IGCAR, Kalpakkam, India
[3]NASA Lewis Research Center
Cleveland, Ohio 44135
[4]Previously, NASA Lewis Research Center
Cleveland, Ohio 44135
Presently, McGaw Technology, Inc.
Fairview Park, Ohio 44126

Abstract

The deformation mechanisms and fatigue behavior of prestrained Inconel 718 superalloy under fully-reversed fatigue were investigated at room temperature. Uniform gage section specimens were monotonically strained initially in either tension or compression up to 2% strain. Fully-reversed fatigue tests were subsequently conducted both on as-machined (no prestrain) and monotonically prestrained specimens in total strain control at a strain range of 0.8%. All tests were conducted in a computer-controlled servohydraulic test system at room temperature. Evolution of stress ranges and mean stresses observed during the fatigue tests on as-machined and prestrained specimens are reported. The specimens were sectioned and examined in a transmission electron microscope to reveal the deformation mechanisms under different types of loading. Results of the investigation and comparisons of the mechanisms of deformation observed under monotonic tensile strain, monotonic compressive strain, fully-reversed fatigue, tensile strain followed by fully-reversed fatigue, and compressive strain followed by fully-reversed fatigue are reported. Fatigue lives of the prestrained specimens are compared with life predictions by two different methods.

Superalloys 718, 625, 706 and Various Derivatives
Edited by E.A. Loria
The Minerals, Metals & Materials Society, 1997

Introduction

The nickel-base, age-hardenable superalloy, Inconel 718 (IN718) is used as a structural material in a wide range of industrial applications. Some examples of the applications within the aerospace industry include gas turbine engine components (1) and powerhead components for the Space Shuttle Main Engine (2). The extensive usage is due primarily to the good mechanical properties (tensile strength, fatigue endurance, and rupture strength), corrosion resistance, and outstanding fabricability (resistance to post-weld cracking) of the superalloy (3). In the past, several investigations were conducted on the metallurgical aspects (4-8), tensile properties (9), fatigue behavior (10-12), and deformation mechanisms (5,6,10,11,13) of the material under monotonic and cyclic loads. More recently, the room temperature fatigue behavior of IN 718 subjected to tensile and compressive prestrains was investigated by Kalluri, Halford, and McGaw (14, 15). The room temperature deformation and damage mechanisms in IN 718 were documented in detail by Kalluri et al. (16) and serrated flow occurring in IN 718 during strain controlled fatigue at room temperature was examined by Bhanu Sankara Rao et al. (17).

In the present study, the deformation mechanisms occurring under monotonic compressive strain, monotonic compressive strain followed by fully-reversed fatigue, and monotonic tensile strain followed by fully-reversed fatigue in IN 718 are reported and compared to one another. Comparisons are also made with previously reported results for monotonic tensile strain, fully-reversed fatigue with no prestrain, and tensile prestrain followed by fully-reversed fatigue conditions. Evolution of the stresses (ranges and means) and the observed fatigue lives for all the conditions are compared. Life is estimated by two models for each fatigue test condition and the results are discussed.

Background

Material

IN 718 used in this study was purchased in the form of wrought bars (31.8 mm dia.). The material was manufactured as per Aerospace Materials Specification 5663D. The chemical composition (weight percent) of the superalloy is as follows: 0.002 S; 0.004 B; 0.006 P; 0.034 C; 0.05 Cu; 0.07 Si; 0.12 Mn; 0.39 Co; 0.57 Al; 0.95 Ti; 2.87 Mo; 5.19 Nb+Ta; 17.52 Cr; 53.58 Ni; balance Fe. The material was solution annealed (1 hr. at 954°C followed by water quenching) and thermally aged (8 hrs. at 718°C followed by furnace cooling to 621°C and 10 hrs. at 621°C) by the manufacturer. Optical microscopy conducted on the as-received material revealed equiaxed grains with an average grain size of 10 μm. At room temperature, the as-received material exhibited the following average tensile properties: a) 0.2% offset yield strength: 1140 MPa, b) ultimate tensile strength: 1410 MPa, and c) percent reduction in cross-sectional area: 43.3 (16).

Metallurgical Aspects

Microstructure of the as-received material was examined with transmission electron microscopy (TEM) and the different phases observed in the alloy were reported in detail previously (16). The main strengthening intermetallic phase in this material is γ'' with a volume fraction of 15-20%. In IN 718, γ'' precipitates coherently as ellipsoidal, disc-shaped particles on {100} planes of the fcc matrix (4-7). Another intermetallic phase, the coherent fcc γ' with a volume fraction of 4% also contributes to the strength of IN 718 (4-6). Needle-shaped precipitates of orthorhombic δ phase and continuous networks of niobium-rich carbides observed on grain boundaries in the as-received material were also previously reported (16).

Mechanical Testing

Test specimens with a uniform gauge section diameter of 6.3 mm were machined from the wrought IN 718 bars. The final polishing marks for all the test specimens were in the longitudinal direction. All the mechanical testing was performed in ambient air at room temperature in a computer-controlled, servohydraulic test system. An extensometer with a gauge length of 12.7 mm was used to measure the strains in the uniform gauge sections of the specimens. Monotonic straining in either tension or compression and fully-reversed fatigue testing were performed with materials testing software (18). Additional details on mechanical testing procedures and comprehensive fully-

reversed, strain-controlled, fatigue data bases generated on as-machined and prestrained (tension or compression) were documented elsewhere (14, 15). The test matrix used for the present investigation is shown in Table I. Initially, specimens were monotonically strained in axial tension or compression to 2%. Fully-reversed fatigue tests were then conducted in axial strain control at a frequency of 1.0 Hz on as-machined and prestrained specimens. A total axial strain range of 0.8% was employed for all the fatigue tests and failure was defined as separation of the test specimen into two pieces. Test conditions and the experimentally observed fatigue lives are indicated in Table I.

Table I Test Matrix and Fatigue Lives

Monotonic Strain Tests, ε_t	Fully-Reversed Fatigue Tests, $\Delta\varepsilon_t$ (N_f)	Fully-Reversed Fatigue Tests on Prestrained Specimens ε_t: $\Delta\varepsilon_t$ (N_f)
0.02	0.008 (363 452 Cycles)	0.02 : 0.008 (34 684 Cycles)
- 0.02	---	- 0.02 : 0.008 (252 363 Cycles)

Results

Evolution of Cyclic Stresses and Fatigue Lives

The stress ranges and mean stresses observed during the fatigue tests on as-machined and prestrained specimens are depicted in Figs. 1 and 2, respectively. The changes in the cross-sectional

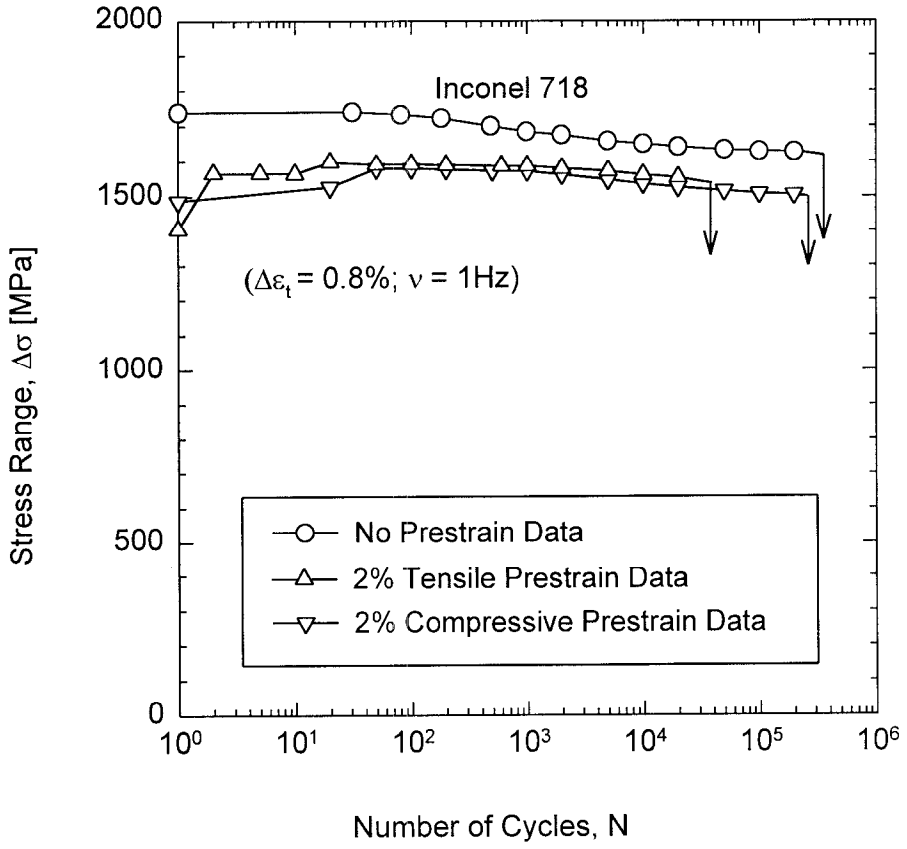

Figure 1 - Evolution of stress ranges in fully-reversed fatigue tests

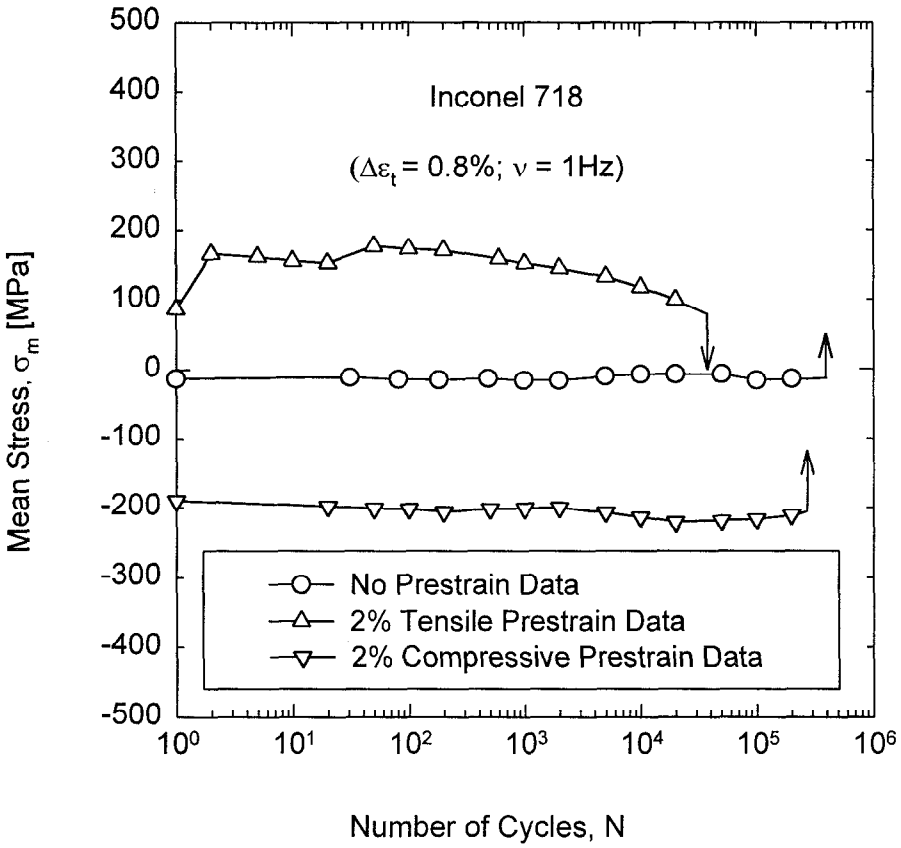

Figure 2 - Evolution of mean stresses in fully-reversed fatigue tests

areas of the prestrained specimens were properly taken into consideration while computing these stresses. In general for a majority of the life, IN 718 in the as-machined and prestrained conditions cyclically softened, however, a small amount of initial hardening occurred in all the specimens. The evolution of stress ranges for both the tensile and compressive prestrained specimens are nearly the same and stress ranges in both the cases are lower than the stress range observed for the as-machined specimen. A similar result was previously observed by Kalluri et al. on a 10% tensile prestrained specimen tested subsequently in fully-reversed fatigue at a strain range of 0.8% (16).

The specimen with no prestrain developed small magnitude compressive mean stresses during fatigue (Fig. 2). However, specimens prestrained both in tension and compression developed mean stresses of large magnitudes during the subsequent fatigue loading. The specimen prestrained in tension exhibited tensile mean stress, whereas the specimen prestrained in compression developed compressive mean stress. The fatigue life of tensile prestrained specimen was lower than that observed for the specimen with no prestrain by more than a factor of 10. The fatigue life of compressively prestrained specimen was not significantly lower than that observed for the specimen with no prestrain. This result is not unexpected because in general tensile mean stress leads to a debit in fatigue life, whereas compressive mean stress generally leads to enhanced fatigue life. In the case of IN 718, even though the compressive mean stress was of the same order of magnitude as the tensile mean stress, which caused a significant debit in fatigue life, no improvement in fatigue life was observed for the compressively prestrained specimen.

Deformation Mechanisms

Samples for TEM investigations were obtained from the gauge sections of the tested specimens. Details of sample preparation were previously reported by Kalluri et al. (16). The deformation mechanisms observed in a specimen deformed to 2% monotonic tensile strain and another

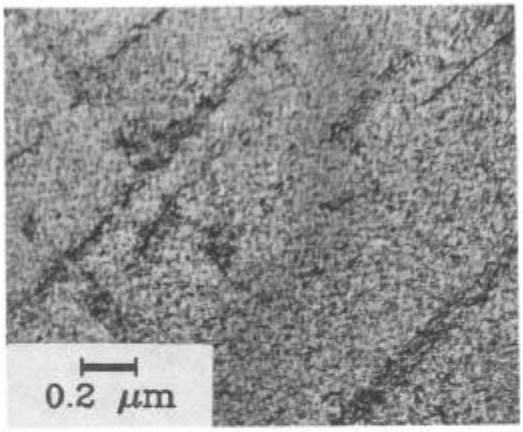

(a) Deformation in multiple planar arrays (from Ref. (16))

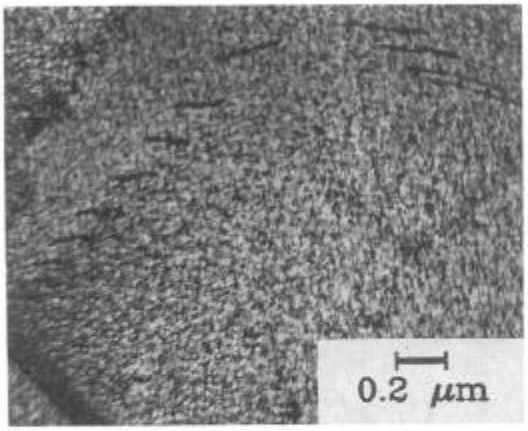

(b) Dislocations and dislocation pairs in planar slip bands (from Ref. (16))

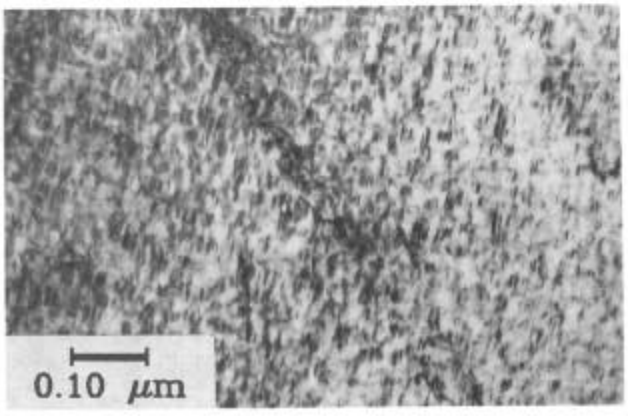

(c) Deformation band and intragranular γ″

Figure 3 - Deformation substructure in monotonic tension, $\varepsilon_t = 2\%$

specimen subjected to 0.8% fully-reversed strain range were also reported earlier (16). However, some of the results are included in this paper for direct comparison with the deformation mechanisms observed under monotonic compression, compressive prestrain followed by fully-reversed fatigue, and tensile prestrain followed by fully-reversed fatigue.

Monotonic Tensile Strain. In the sample subjected to 2% tensile strain, deformation in multiple planar arrays (Fig. 3a), dislocations, and dislocation pairs (generally associated with γ″ particles; Fig. 3b) were previously (16) reported. Presence of dislocation pairs, which was also observed by Oblak et al. (5) and Chaturvedi and Han (6) is an indication of shearing of ordered particles (γ″) by glide dislocations (6). Closer examination of the sample clearly revealed active interaction between the deformation bands and intragranular γ″ (Fig. 3c).

Monotonic Compressive Strain. Deformation in planar arrays (Fig. 4a) and dislocations in the vicinity of a network of niobium-rich carbides near a grain boundary (Fig. 4b) were observed in the sample subjected to 2% compressive strain. In addition, dislocation tangles in the matrix (regions between deformation bands; Fig. 4c) and dislocations adjacent to the grain boundaries (Fig. 4d) were noticed. The dislocations near the grain boundaries appeared to be almost parallel to the grain boundaries. Such a dislocation arrangement was not observed in the sample subjected to 2% monotonic tensile strain and its significance is discussed later in the paper.

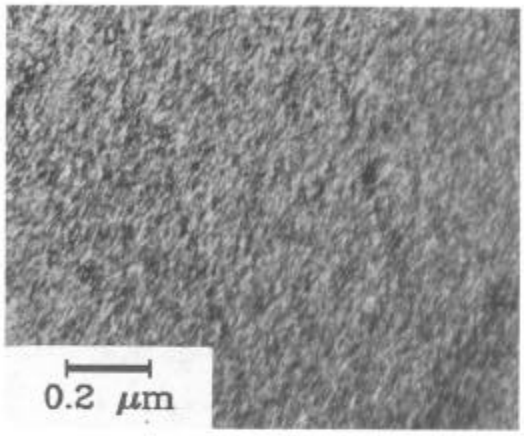

(a) Deformation in planar arrays

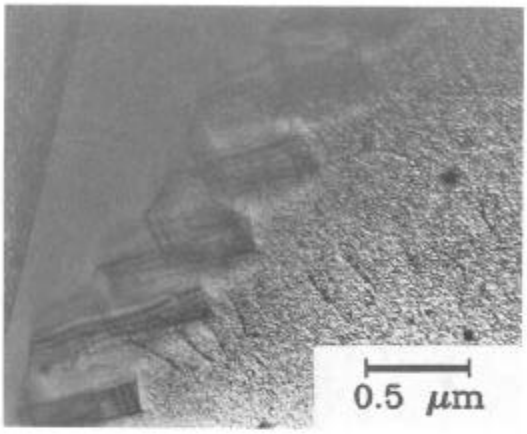

(b) Dislocations in the vicinity of a network of niobium-rich carbides near a grain boundary

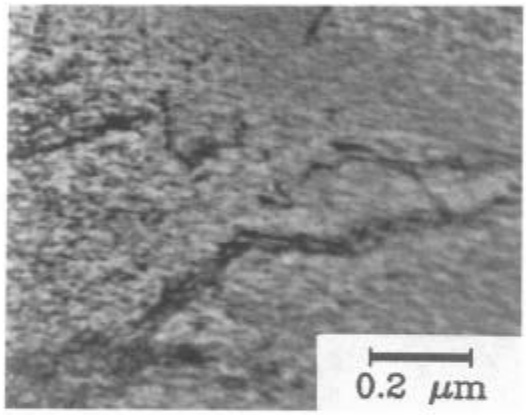

(c) Dislocation tangles in the regions between deformation bands

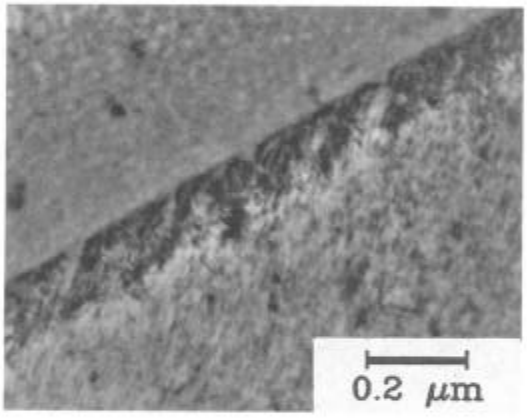

(d) Dislocations adjacent to a a grain boundary

Figure 4 - Deformation substructure in monotonic compression, ε_t = -2%

Fully-Reversed Fatigue (No Prestrain). In the specimen fatigued at a strain range of 0.8%, dislocation pairs (evidence of γ″ shearing), pile-up of dislocations near grain boundaries, and co-planar slip were previously observed (Figs. 5a and 5b). A well-defined slip band that continued into an adjacent twin across the boundary was also noticed in the same specimen (Fig. 5c). At room temperature under fatigue, the deformation in IN 718 predominantly occurs in planar slip bands after initial shearing of γ″ particles. Successive shearing of the γ″ particles during subsequent cycling tends to reduce their size and decreases the resistance offered by these particles to the movement of dislocations within the slip band (16). The trailing dislocations in the slip band are less likely to encounter any ordered γ″ and this mechanism leads to a planar arrangement of dislocations within the slip band (Fig. 5a and 5c). Such planar arrangement dislocations was reported by Bhanu Sankara Rao et al. (17) in solution annealed IN 718 (which is devoid of any γ″ particles) tested at room temperature in strain-controlled fatigue. Some deformation bands in the fatigue specimen tested at a strain range of 0.8% did not contain any discernible γ″ particles (Fig. 5d). Planar slip and precipitate-free deformation bands were also observed by other investigators in IN 718 tested at room temperature in fatigue (10, 11, 13). The cyclic softening observed during fatigue testing of as-machined and prestrained specimens is due to the "mechanical scrambling" of the γ″ precipitates within the slip bands (16).

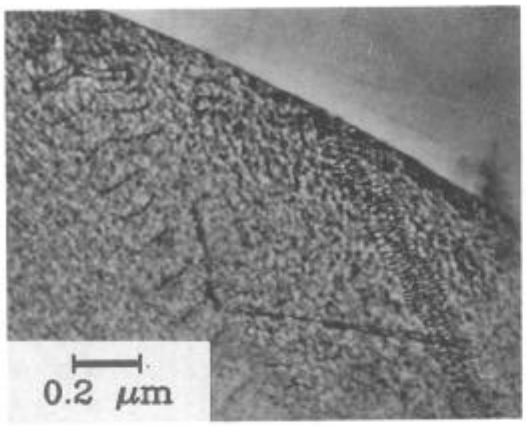

(a) Dislocation pairs, slip band, and pile-up at a grain boundary

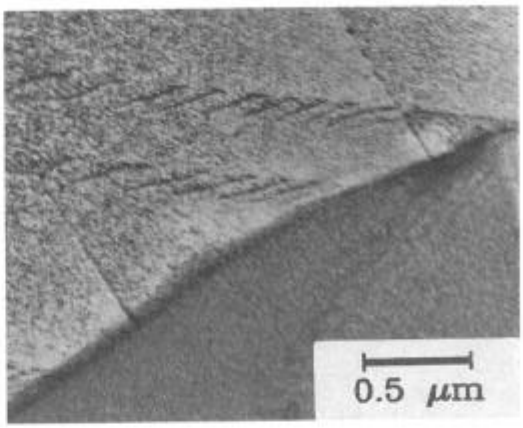

(b) Co-planar slip and dislocation pile-up

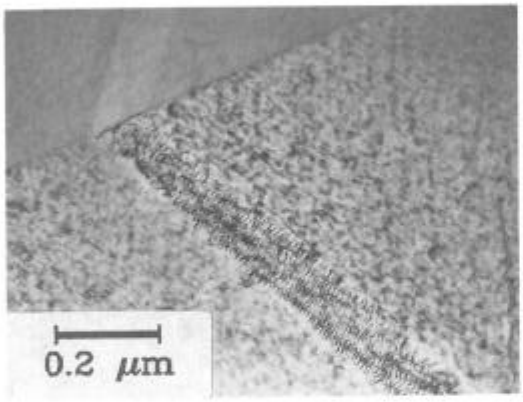

(c) Slip band continuation into an adjacent twin

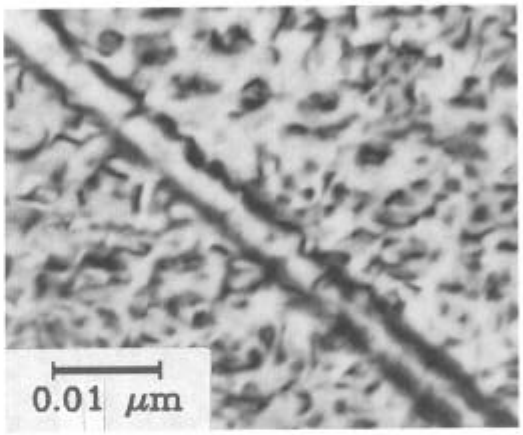

(d) Precipitate-free deformation band

Figure 5 - Substructure in specimen tested under fully-reversed fatigue without prestrain, $\Delta\varepsilon_t = 0.8\%$ (from Ref .(16))

Tensile Prestrain Followed by Fatigue. In the specimen tested at a strain range of 0.8% after a prior tensile deformation of 2%, well-defined, co-planar slip bands (Fig. 6a) and deformation in multiple planar arrays (Fig. 6b) were observed. The regions between the slip bands were relatively free of any dislocations or dislocation tangles indicating that the deformation during the subsequent fatigue portion of the test was confined primarily to the deformation bands activated during the tensile prestrain.

Compressive Prestrain Followed by Fatigue. Deformation bands with dislocations tangles (Fig. 7a) and dislocations and dislocation pairs (Fig. 7b) were observed in the specimen tested at a strain range of 0.8% after a compressive prestrain of 2%. The presence of dislocation pairs indicates that the γ' shearing mechanism is activated during the subsequent fatigue cycling. As in the case of the specimen subjected to 2% monotonic compression, dislocation tangles in the regions between deformation bands (Fig. 7c) and dislocations in the vicinity of a grain boundary were also observed (Fig. 7d). The deformation substructure created by the monotonic compression appears to prevail even after subsequent fatigue cycling.

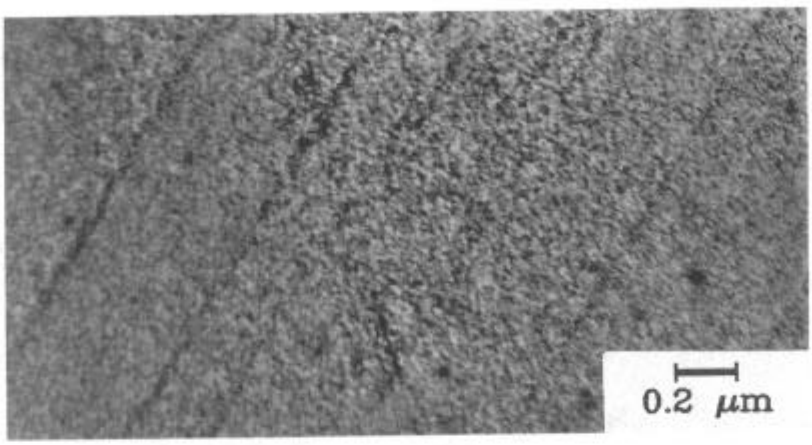

(a) Well-defined, co-planar slip bands

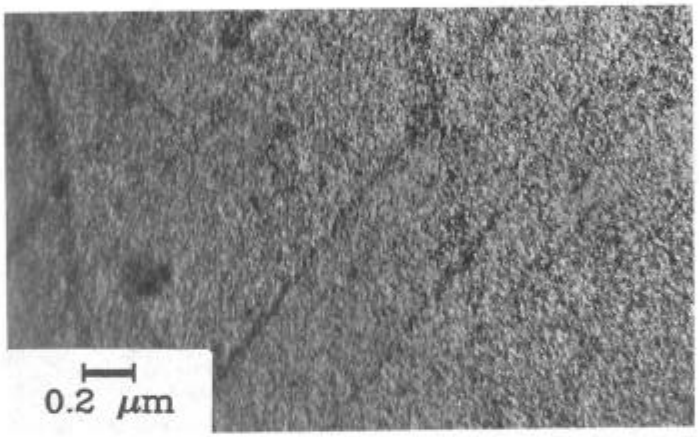

(b) Deformation in multiple planar arrays

Figure 6 - Substructure in specimen tested under fatigue after 2% tensile prestrain, $\Delta\varepsilon_t = 0.8\%$

Fatigue Life Prediction

Procedures for estimating the fatigue lives of prestrained specimens and degree of accuracy of different life prediction methods were documented in detail by Kalluri, Halford, and McGaw (14, 15). Fatigue life estimations for the two prestrained specimens (deformation substructures of which have been discussed in previous sections) are included in this paper. Fatigue lives of prestrained specimens were estimated with a Linear Damage Rule (LDR; Ref. 19) and a nonlinear Damage Curve Approach (DCA; Ref. 20). The influence of mean stress on fatigue life was taken into consideration by the Smith, Watson, and Topper (SWT) parameter (21). The mathematical formulations and implementation techniques for all the life prediction methods were reported in Ref. 15. The estimated fatigue lives are shown in Table II for the prestrained specimens.

Table II Estimation of Fatigue Lives[5] of the Prestrained Specimens

ε_t: $\Delta\varepsilon_t$	Experiment	LDR	DCA	LDR&SWT	DCA&SWT
0.02 : 0.008	34 684	294 630	122 270	118 273	63 646
- 0.02 : 0.008	252 363	326 037	130 156	4 342 398	718 383

[5]Number of cycles.

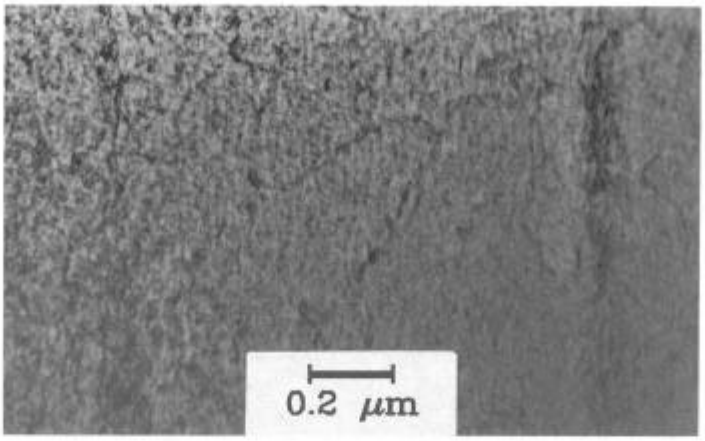

(a) Deformation bands with dislocation tangles

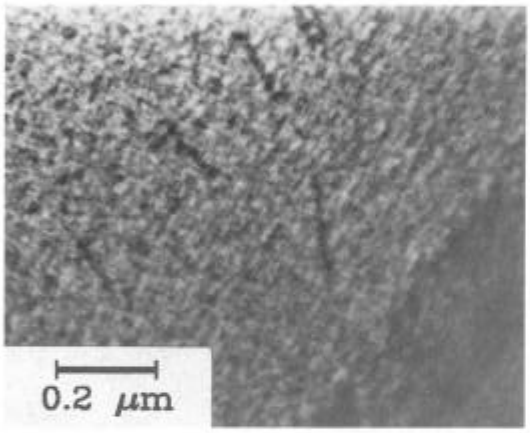

(b) Dislocations and dislocation pairs

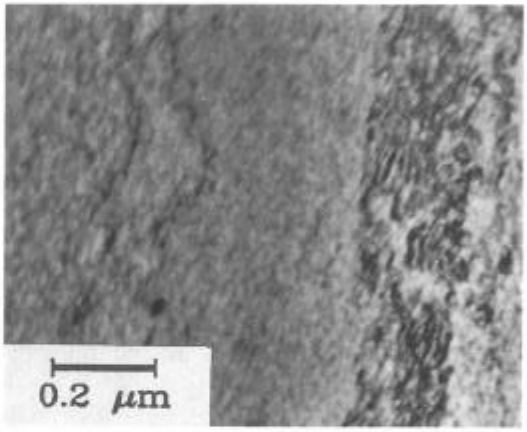

(c) Dislocation tangles in the matrix region and a deformation band

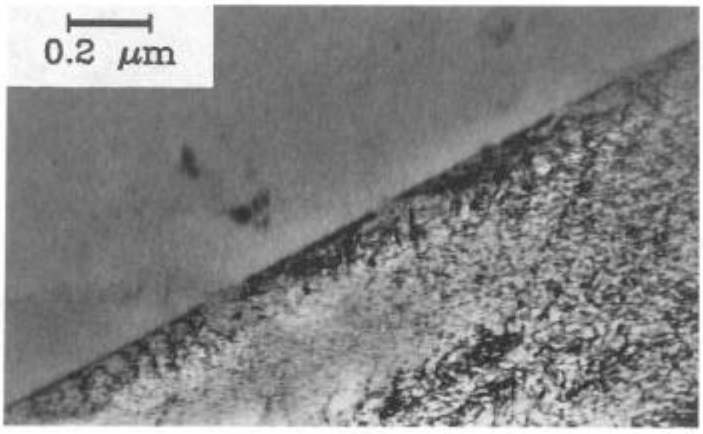

(d) Dislocations in the vicinity of a grain boundary

Figure 7 - Substructure in specimen tested under fatigue after 2% compressive prestrain, $\Delta\varepsilon_t = 0.8\%$

Fatigue lives were estimated both without (columns LDR and DCA in Table II) and with (columns LDR&SWT and DCA&SWT) the consideration of mean stress effects. In the case of the tensile prestrained specimen, the best life prediction was obtained by the DCA&SWT method. However, fatigue lives estimated by LDR and DCA methods were within a factor of two of the experimentally observed life for the specimen prestrained in compression.

Discussion

At room temperature, under monotonic tension and compression, deformation occurred in planar arrays in IN 718. Dislocation pairs observed under monotonic tension are generated when two glide dislocations pass successively through ordered γ'' precipitates (5,6,16). Selective pathways for the movement of dislocations are established within a slip band as more γ'' precipitates are sheared with additional deformation. Such a localization of dislocations in slip bands under monotonic tension can lead to inhomogeneous deformation. Under monotonic compression, other deformation mechanisms such as dislocation tangles in the regions between deformation bands and dislocations near grain boundaries were also noticed. These observations indicate that deformation under monotonic compression is not as inhomogeneous as that observed under monotonic tension.

Under fully-reversed fatigue without any prestrain, passage of dislocations within the slip bands tends to continuously shear the strengthening γ'' precipitates in IN 718 and as a consequence reduce their size with additional cycling. This phenomenon identified as "mechanical scrambling" of γ'' precipitates by Kalluri et al. (16) causes the observed cyclic softening and leads to the precipitate-free deformation bands. Cycling softening in precipitate-strengthened superalloys (Waspaloy and Nimonic 80A) due to shearing of precipitates (22) and precipitate-free deformation bands in IN 718 (10,11,13) were reported by other investigators. The lower stress ranges observed in fatigue tests on the 2% prestrained specimens (Fig. 1) are a consequence of the shearing of γ'' precipitates in a few selective slip bands during the prior monotonic strains. In the tensile prestrained specimen tested subsequently in fatigue, the deformation was very inhomogeneous and was confined mainly to the well-defined deformation bands activated during prestraining. Such a localization of deformation can cause stress concentration regions near grain boundaries due to dislocation pile-ups and these regions can evolve into crack initiation sites, thus lowering the fatigue life of the specimen. The observed fatigue life of the tensile prestrained specimen was indeed lower by more than a factor of 10 than that observed for the specimen with no prestrain (Table I). Even though γ'' shearing mechanism was active in the compressively prestrained specimen tested subsequently in fatigue, the deformation was not confined only to well-defined slip bands. Evidence of dislocation tangles in the regions between deformation bands and presence of dislocations along the grain boundaries indicate that deformation in the compressively prestrained specimens is more homogenous compared to the tensile prestrained specimen. This additional homogenous deformation reduces the propensity for the occurrence of stress concentration regions and crack initiation sites, which translates into a lower debit on fatigue life. In fact, the fatigue life of the compressively prestrained specimens was not significantly lower than that observed for the specimen with no prestrain.

The prestrains investigated in the present study simulate those imposed on the materials during proof testing, accidental overload, or autofrettage. Their influence on subsequent fatigue life is likely to be different from that resulting from the prestrain imposed during cold working, for example, by swaging. In the present study, the mean stresses generated during fatigue in a prestrained specimen were dictated by the direction of the initial prestrain. Tensile mean stress observed for the tensile prestrained specimen reduced the fatigue life by more than a factor of 10, whereas the compressive mean stress observed for the compressively prestrained specimen did not reduce the fatigue life in a significant manner (Table I). For the tensile prestrained specimen, fatigue life predictions without mean stress consideration were unconservative (Table II). A combination of the DCA & SWT method provided the best life prediction indicating that both nonlinear damage accumulation and tensile mean stress influence must be considered for realistic life estimations. Life predictions by LDR and DCA without any consideration for the mean stress influence were within a factor of two for the compressively prestrained specimen. However, for the same specimen inclusion of the mean stress effect through the SWT parameter yielded very unconservative estimates of fatigue life, which indicates the SWT overestimates the beneficial influence of compressive mean stress on fatigue life. For accurate fatigue life predictions, the

influences of tensile and compressive mean stresses on the fatigue life of IN 718 need to be properly characterized.

Conclusions

The conclusions drawn from the present study on Inconel 718 at room temperature under monotonic tension, monotonic compression, and fully-reversed fatigue on as-machined, tensile and compressively prestrained specimens are as follows:

1) Deformation in In 718 under monotonic tension and compression occurred by planar arrays. Presence of dislocation pairs indicated shearing of γ'' precipitates as an active mechanism. Under monotonic tension deformation was more inhomogeneous than under monotonic compression, where dislocation tangles in the regions between deformation bands and dislocations near grain boundaries were observed.

2) In fatigue of as-received and prestrained specimens, deformation occurred primarily by co-planar slip. Cyclic softening observed during fully-reversed fatigue is due the repeated "mechanical scrambling" of γ'' precipitates, which reduces their size and consequently the resistance offered to dislocation movement in slip bands. The observed reduction in the fatigue life of the tensile prestrained specimen compared to the fatigue life of the as-machined specimen is attributed to inhomogeneous deformation that increases the materials susceptibility to microcracking. The deformation in the compressively prestrained specimen was relatively more homogeneous, which reduces the propensity for microcracking, and the fatigue life of the specimen was only slightly lower than that observed for the specimen with no prestrain.

3) Realistic estimation of fatigue life after prestraining requires a nonlinear fatigue damage accumulation model and a technique to account for the influences of both tensile and compressive mean stresses on fatigue life.

Acknowledgements

S. Kalluri wishes to thank Dr. Ivan E. Locci, Resident Research Associate, NASA Lewis Research Center for many insightful discussions. K. Bhanu Sankara Rao wishes to acknowledge National Research Council, Washington, DC for granting the associateship award. The diligent efforts of Mr. Christopher S. Burke, NYMA, Inc., in the fatigue laboratory at NASA Lewis Research Center are gratefully acknowledged.

References

1. D. D. Krueger, "The Development of Direct Age 718 for Gas Turbine Engine Disk Applications," Superalloy 718 - Metallurgy and Applications, ed. E. A. Loria (Warrendale, PA: The Minerals, Metals & Materials Society, 1989), 279-296.

2. R. P. Jewett and J. A. Halchak, "The Use of Alloy 718 in the Space Shuttle Main Engine," Superalloys 718, 625 and Various Derivatives, ed. E. A. Loria (Warrendale, PA: The Minerals, Metals & Materials Society, 1991), 749-760.

3. "Inconel Alloy 718," (Huntington, WV: Inco Alloys International, Inc., 1985), 1-24.

4. D. F. Paulonis, J. M. Oblak, and D. S. Duvall, "Precipitation in Nickel-Base Alloy 718," Trans. ASM, 62 (1969), 611-622.

5. J. M. Oblak, D. F. Paulonis, and D. S. Duvall, "Coherency Strengthening in Ni Base Alloys Hardened by DO_{22} γ'' Precipitates," Met. Trans, 5 (1974), 143-153.

6. M. C. Chaturvedi and Y. Han, "Strengthening Mechanisms in Inconel 718 Superalloy," Metal Science, 17 (1983), 145-149.

7. J. W. Brooks and P. J. Bridges, "Metallurgical Stability of Inconel Alloy 718," Superalloys 1988, ed. S. Reichman et al., (Warrendale, PA: The Metallurgical Society, 1988), 33-42.

8. A. Oradei-Basile and J. F. Radavich, "A Current T-T-T Diagram for Wrought Alloy 718," Superalloys 718, 625 and Various Derivatives, ed. E. A. Loria (Warrendale, PA: The Minerals, Metals & Materials Society, 1991), 325-334.

9. G. E. Korth and C. L. Trybus, "Tensile Properties and Microstructure of Alloy 718" Superalloys 718, 625 and Various Derivatives, ed. E. A. Loria (Warrendale, PA: The Minerals, Metals & Materials Society, 1991), 437-446.

10. H. F. Merrick, "The Low Cycle Fatigue of Three Wrought Nickel-Base Alloys," Met. Trans, 5 (1974), 891-897.

11. D. Fournier and A. Pineau, "Low Cycle Fatigue Behavior of Inconel 718 at 298 K and 823 K," Met. Trans, 8A (1977), 1095-1105.

12. G. E. Korth, "Effects of Various Parameters on the Fatigue Life of Alloy 718," Superalloys 718, 625 and Various Derivatives, ed. E. A. Loria (Warrendale, PA: The Minerals, Metals & Materials Society, 1991), 457-476.

13. D. W. Worthem et al., "Cyclic Deformation and Damage Structure in Inconel 718," Biaxial and Multiaxial Fatigue, EGF 3, ed. M. W. Brown and K. J. Miller (London, UK: Mechanical Engineering Publications, 1989), 131-143.

14. S. Kalluri, G. R. Halford, and M. A. McGaw, "Fatigue Behavior of Inconel 718 Superalloy Subjected to Monotonic Tensile and Compressive Strains," (Paper presented at the 1994 Conference on Advanced Earth-to-Orbit Propulsion Technology, NASA-Marshall Space Flight Center, Huntsville, Alabama, 17-19 May 1994).

15. S. Kalluri, G. R. Halford, and M. A. McGaw, "Prestraining and Its Influence on Subsequent Fatigue Life," Advances in Fatigue Lifetime Predictive Techniques: 3rd Volume, ASTM STP 1292, ed. M. R. Mitchell and R. W. Landgraf, (West Conshohocken, PA: American Society for Testing and Materials, 1996), 328-341.

16. S. Kalluri et al., "Deformation and Damage Mechanisms in Inconel 718 Superalloy," Superalloys 718, 625 and Various Derivatives, ed. E. A. Loria (Warrendale, PA: The Minerals, Metals & Materials Society, 1994), 593-606.

17. K. Bhanu Sankara Rao et al., "Serrated Flow and Deformation Substructure at Room Temperature in Inconel 718 Superalloy During Strain Controlled Fatigue," Scripta Metallurgica et Materialia, 32 (4) (1995), 493-498.

18. M. A. McGaw and P. J. Bonacuse, "Automation Software for Materials Testing Laboratory," Applications of Automation Technology to Fatigue and Fracture Testing, ASTM STP 1092, ed. A. A. Braun, N. E. Ashbaugh, and F. M. Smith, (West Conshohocken, PA: American Society for Testing and Materials, 1990), 211-231.

19. M. A. Miner, "Cumulative Damage in Fatigue," Journal of Applied Mechanics, 67 (1945), A159-A164.

20. S. S. Manson and G. R. Halford, "Practical Implementation of the Double Linear Damage Rule and Damage Curve Approach for Treating Cumulative Fatigue Damage," International Journal of Fracture, 17 (2) (1981), 169-192.

21. K. N. Smith, P. Watson, and T. H. Topper, "A Stress-Strain Function for the Fatigue of Metals," Journal of Materials, 5 (4) (1970) 767-778.

22. S. D. Antolovich and B. Lerch, "Cyclic Deformation, Fatigue and Fatigue Crack Propagation in Ni-base Alloys," Superalloys, Supercomposites and Superceramics, (Academic Press, Inc., 1989), 375.